# Design of soil moisture distribution sensor based on high-frequency capacitance

Yan Hua[1,2], Tang Zejun[1*], Xing Zhen[2], Gao Dingneng[1], Hong Haoxing[2]

(1. *College of Water Conservancy and Civil Engineering, China Agricultural University, Beijing 100083, China*;
2. *National Engineering Research Center for Information Technology in Agriculture, Beijing 100097, China*)

**Abstract:** In order to obtain accurate real-time soil moisture data and the spatial distribution of soil moisture, the soil moisture measurement methods based on high-frequency capacitance edge field effect were analyzed, the structure of probe was studied, and a multi-channel soil moisture sensor was designed. Moreover, with the established two-dimensional trace planar capacitance probe model and the method of the finite element analysis, relationship between the structure of sensor probe and electric field intensity was studied and capacitance of the probe trace amount planar capacitance model was analyzed, the most optimal structure of sensor probe was determined. Design parameters of the probe which can achieve optimal sensitivity and detection range are: outer diameter 40 mm and inner diameter 38.4 mm for the probe copper ring electrode, axial length 20 mm and axial spacing 10 mm. The sensor is suitable for measuring the moisture of different type of soil. Moreover, the features of the profile soil moisture sensor were experimentally explored. The measurement accuracy reached ±1.31% with better stability and consistency. Sensor probes can be assembled according to the measurement depth and used to measure soil moisture of different crop root zone.

**Keywords:** high frequency capacitance detection, profile, soil moisture sensor

**DOI:** 10.3965/j.ijabe.20160903.2226

**Citation:** Yan H, Tang Z J, Xing Z, Gao D N, Hong H X. Design of soil moisture distribution sensor based on high-frequency capacitance. Int J Agric & Biol Eng, 2016; 9(3): 122－129.

## 1 Introduction

Real-time and accurate soil moisture data of farmland are very important for studying the law of soil moisture movement and crop moisture stress, implementing water-saving irrigation and improving agricultural production benefits[1,2]. Various soil moisture measurement methods, such as oven drying method, tension meter method, neutron method, resistance method, and dielectric method have already been developed[3,4]. Nowadays, measuring methods based on dielectric theory[5-9] is widely used due to its advantages of high precision, real-time measurement, and convenient setting. With the development of precision agriculture, it is necessary to study the migration process of soil moisture[10,11], water absorption rule in crop root zone[12], and soil moisture gradient change with soil depth. In the above study fields, the measurement of moisture change of soil profile is required. Currently, the most widely used soil moisture sensor is the probe type and the probe length is usually less than 30 cm. It is mainly used to measure the moisture of soil by surface or single point. Among the common moisture measurement methods of profile soil, most of the probes needed to be inserted into different depths of soil. The measurement process is time-consuming and had, commonly leads to soil structure damages and different sensors have different measurement results. The moisture measurements of

**Received date:** 2015-11-03 **Accepted date:** 2016-03-13

**Biographies: Yan Hua,** PhD, Associate professor, research interests: water conservancy information technology and application, Email: yanh@nercita.org.cn; **Xing Zhen,** Master, research interests: mechanical design and theory, Email: xingz@nercita.org.cn; **Gao Dingneng,** Master, research interests: water resources and water environment, Email: 1654722462@qq.com; **Hong Haoxing,** B.S., research interests: information and computing science, Email: honghx@nercita.org.cn.

***Corresponding author: Tang Zejun,** PhD, Professor, research interests: hydrology and water resources. Mailing address: PO Box 104, China Agricultural University (East Campus) Tsinghua East Road 17#, Beijing 100083, China. Tel: +86 62737874, Email: tangzejun@sina.com.

soil profile[13,14] have been extensively studied abroad in recent years. However, the related application was seldom explored in China.

In this research, we analyzed the high-frequency capacitance edge field effect[15,16] and designed and manufactured a profile soil moisture sensor based on high-frequency capacitance. Moreover, we explored the structure of the sensor probe and the overall structure of profile sensor. Through the field experiment, we verified the precision, stability and consistency of the sensor.

## 2 Measuring principle

Soil is a porous medium composed of three states: solid, liquid and gas. The relative dielectric constants of water, solid soil and air are 81, 3-5 and 1 respectively. Therefore, the dielectric constant of water is much larger than that of other substances in the soil. This property can be used to measure soil water percentage indirectly and method to measure soil moisture percentage based on edge field effect of high-frequency capacitance introduced in this research is based on the above property.

The measurement mechanism of the sensor developed was based on the edge field effect of high-frequency capacitance. The annular sensing electrode acted as the capacitance component of high frequency circuit and the surrounding soil acted as the dielectric medium. The relative dielectric constant of the soil changes with the change of soil water percentage, thus this leads to the change of capacitance value sensed by sensor prob. The change in the capacitance value further leads to the frequency change of oscillation circuit. Therefore, we can indirectly measure soil volumetric water percentage by measuring output frequency of high-frequency oscillator.

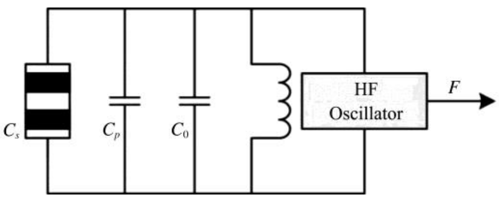


Figure 1 Measurement principle of the sensor probe

As is shown in Figure 1, the /output frequency of high-frequency oscillation circuit can be calculated as:

$$F = \frac{1}{2\pi\sqrt{L_0(C_s + C_p + C_0}} \quad (1)$$

where, $L_0$ is inductance of oscillation circuit; $C_0$ is matching capacitance for ensuring the normal vibration of the circuit; $C_p$ is parasitic capacitance of the circuit; $C_s$ is soil equivalent capacitance sensed by the probe.

The capacity of soil equivalent capacitance sensed by the probe is related to the soil around probe and the parasitic capacitance of probe itself:

$$Cs = k\varepsilon \quad (2)$$

where, $\varepsilon$ is the relative dielectric constant of soil; $k$ is related to the structure of probe.

According to Equations (1) and (2), let $A = \frac{1}{2\pi^2 kL_0}$ and $B = -\frac{C_p + C_0}{k}$, then:

$$\varepsilon = AF^{-2} + B \quad (3)$$

where, $A$ and $B$ are parameters related to probe structure. Therefore, if the size of probe is known, the dielectric constant of the soil is only related to the output frequency of the sensor. The volumetric water percentage of the soil can be calculated according to the TOPP Equation[17]: $\theta_v = -5.3\times10^{-2}+2.92\times10^{-2}\varepsilon-5.5\times10^{-4}\varepsilon^2+4.3\times10^{-4}\varepsilon^3$.

## 3 Design and analysis of the sensor structure

### 3.1 Sensor structure

The overall structure of the profile sensor is shown in Figure 2. It consists of the probe, detection body and protective sleeve. The detection body could be assembled with the probe according to the actual measurement depth. The physical connection among probes was realized via internal and external screw threads and the electrical connection was realized via electric contact. As an important part of the sensor, the protective sleeve was made by PVC material. The protection grade reached IP68.

a. Probe b. Detection body c. Protective sleeve

Figure 2 Sensor structure

### 3.2 Modeling analysis of probe structure

As is shown in Figure 3, the sensor probe is composed of two circular rings: ID = 19.2 mm, OD = 20 mm, the axial length *a*, and the axial distance between the two rings *b*. In order to analyze the relationship between the electromagnetic field distribution around the probe and the probe structure, optimize the probe structure, and determine the parameters *a* and *b*, the finite element analysis method was adopted. The sensor probe was divided into 126 parts along the circumference, and the width of each part was 1 mm. The longitudinal sections (shadow) of each circle were selected to constitute a micro-scale planar capacitance and the total soil capacitive reactance sensed by the whole probe was equivalent to that sensed by the sum of 126 parallel micro-scale capacitances.

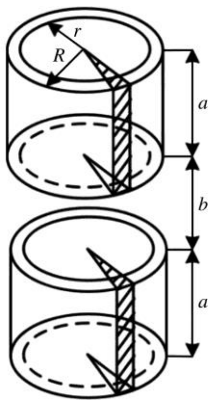


Figure 3 Physical model of the probe

Two-dimensional model of the micro-scale planar capacitance was established with Maxwell V10, the finite element analysis software developed by Ansoft Company. We analyzed the changing tendency of electric field intensity and the energy distribution rule around the micro-scale planar capacitance. The two-dimensional model of micro-scale planar capacitance is shown in Figure 4. The length of the drive electrode and the sensing electrode is set as *a*; the distance between them is set as *b*; *H* is the soil height above the probe, 60 mm; length *L* is 2*a*+*b*+10 mm; the lower part of the electrode is the base with the thickness of *a*+*b*. The base thickness is equal to the distance between the centers of two electrodes and the guard electrode is set below them[18]. In order to reduce the influence of the parasitic capacitance, the guard electrode and the sensing electrode only work when the excitation source is loading in[19].

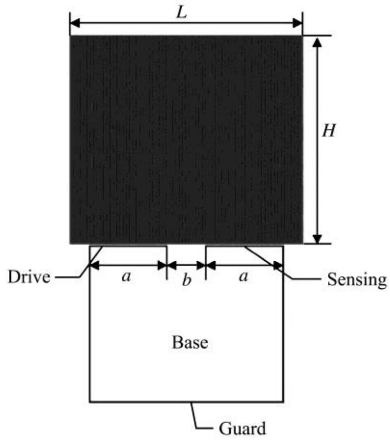


Figure 4 Two-dimensional model of micro-scale planar capacitor

After establishing the two-dimensional model, the sine wave voltage was loaded on the drive electrode. The range and frequency of the voltage was respectively 5 V and 100 MHz. The sensing electrode and the guard electrode were connected to the ground. The electrode material is copper and the base material is PVC. The dielectric constant of the PVC is 3.2. The space outside the model is a vacuum. The boundary conditions were set as “ballon”. The solver was set as the electric field and the solving parameters included the electric field intensity and capacitance. The margin of error of solver was controlled within 1e-5 through the adaptive control mode and the twice iterative error was set as 0.02%. Then the electric field distribution around the micro-scale planar capacitance (Figures 5 and 6) and the value of the micro-scale planar capacitance (Tables 1 and 2) could be respectively calculated through changing the size of copper ring (*a* and *b*) and the dielectric constant of the soil.

As is shown in Figure 5, the corresponding electric field intensity decreases gradually when *b* is 10 mm and *a* is less than 20 mm. When *a* is 20 mm, the corresponding electric field intensity is smallest. If *a* is longer than 20 mm, the corresponding electric field intensity increases gradually. Because the square of the electric field intensity is inversely proportional to the corresponding electric place size under the same electric field energy, therefore, when *a* is 20 mm, the electric field intensity is smallest and its corresponding area is largest. We can also be intuitive to see from the graph that the electric field distribution area is the largest in Figure 4, and the detection range is the largest.

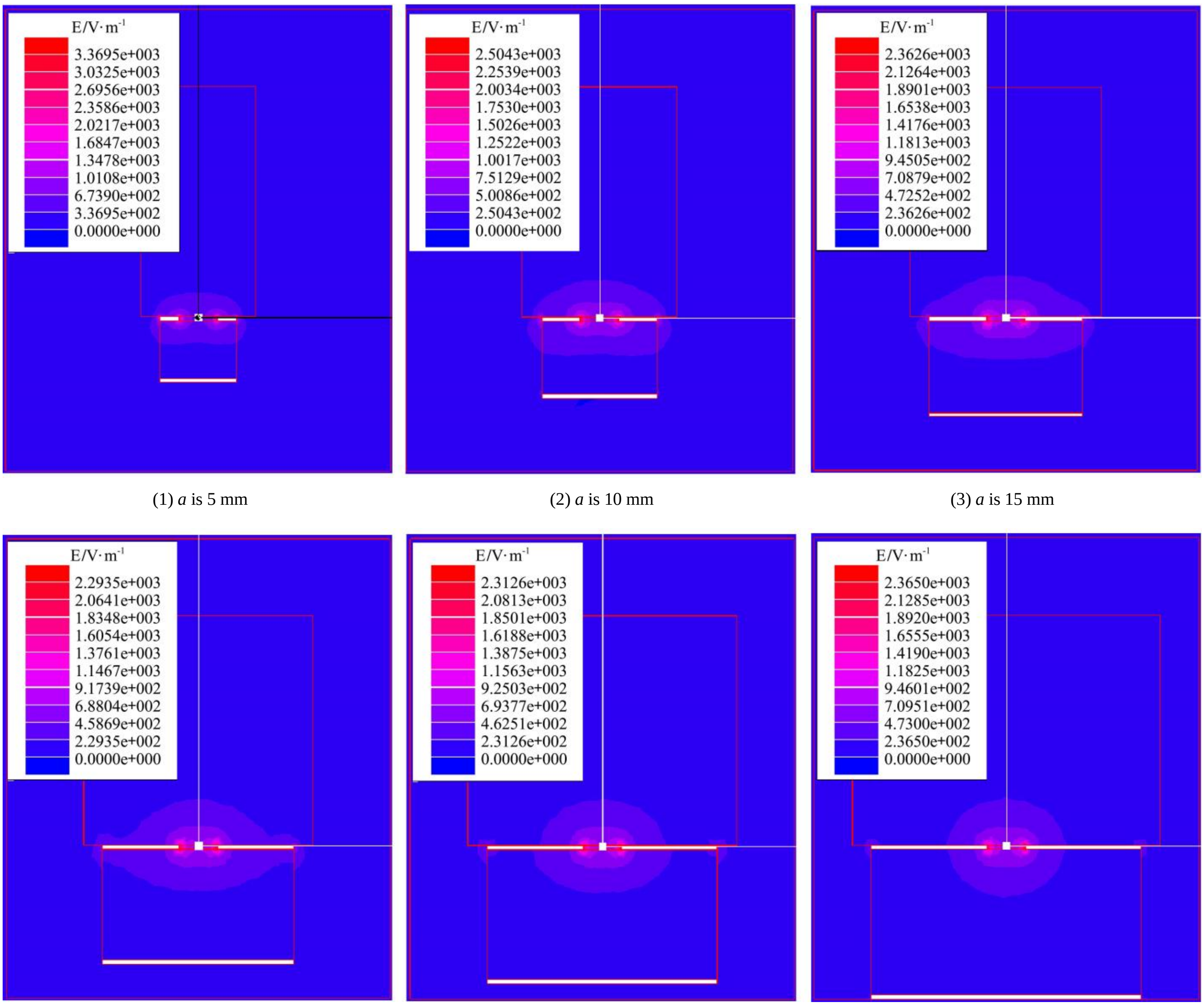


(1) *a* is 5 mm (2) *a* is 10 mm (3) *a* is 15 mm

(4) *a* is 20 mm (5) *a* is 25 mm (6) *a* is 30 mm

Figure 5 Electric field distributions around micro-scale planar capacitance when b is 10 mm and ε is 3.2

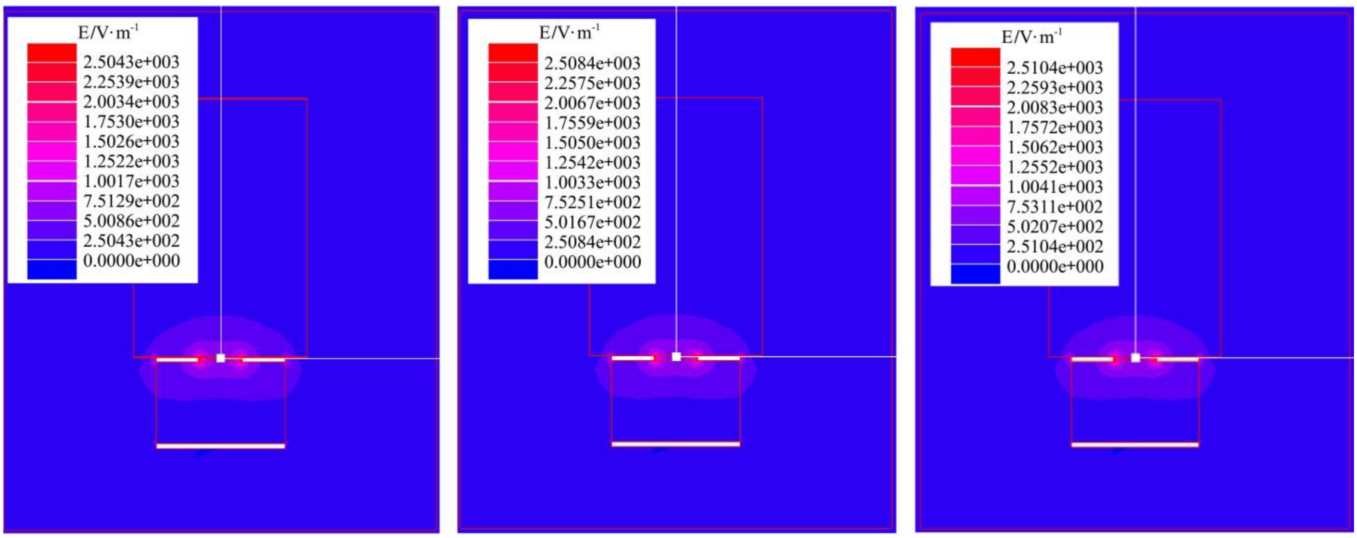


(1) $\varepsilon=3.2$ (2) $\varepsilon=10.2$ (3) $\varepsilon=43.6$

Figure 6 Electric field distribution around the micro-scale planar capacitance under different dielectric constants

When the values of *a* and *b* keep unchanged, electric field distribution around the micro-scale planar capacitance under different dielectric constants is shown in Figure 6. With different dielectric constants, the electric field energy around the micro-scale planar capacitance of the probe and the corresponding detection range stay the same. According to the analysis above, the sensor can be applied to moisture measurements of different soil types.

**Table 1 Capacity values of micro-scale planar capacitance of probe for different *a*/*b* ratios and different dielectric constants**

Unit: *p*F

| *a*/*b* | $\varepsilon_1$=3.2 | $\varepsilon_2$=6.3 | $\varepsilon_3$=10.2 | $\varepsilon_4$=16.8 | $\varepsilon_5$=20.3 | $\varepsilon_6$=25 | $\varepsilon_7$=43.6 |
|---|---|---|---|---|---|---|---|
| 0.5 | 74.3 | 107.1 | 149.0 | 220.5 | 258.6 | 309.8 | 513.0 |
| 1 | 90.0 | 129.7 | 180.2 | 266.3 | 312.0 | 373.6 | 617.7 |
| 1.5 | 99.8 | 143.6 | 199.2 | 293.8 | 344.2 | 411.9 | 680.3 |
| 2 | 107.9 | 154.9 | 214.5 | 315.8 | 369.7 | 442.2 | 729.2 |
| 2.5 | 116.2 | 165.2 | 227.6 | 333.5 | 389.9 | 465.7 | 766.3 |
| 3 | 118.5 | 169.6 | 234.2 | 343.9 | 402.1 | 480.5 | 790.9 |

**Table 2 Adjacent capacity differences of micro-scale planar capacitance of the probe**

Unit: *p*F

| *a*/*b* | $C_2$-$C_1$ | $C_3$-$C_2$ | $C_4$-$C_3$ | $C_5$-$C_4$ | $C_6$-$C_5$ | $C_7$-$C_6$ |
|---|---|---|---|---|---|---|
| 0.5 | 32.8 | 41.9 | 71.5 | 38.1 | 51.2 | 32.8 |
| 1 | 39.7 | 50.5 | 86.1 | 45.7 | 61.6 | 39.7 |
| 1.5 | 43.8 | 55.6 | 94.6 | 50.4 | 67.7 | 43.8 |
| 2 | 47 | 59.6 | 101.3 | 53.9 | 72.5 | 47 |
| 2.5 | 49 | 62.4 | 105.9 | 56.4 | 75.8 | 49 |
| 3 | 51.1 | 64.6 | 109.7 | 58.2 | 78.4 | 51.1 |

As shown in Table 1, when ratio of *a*/*b* is constant, the capacity value of the micro-scale planar capacitance increases gradually with the increase of dielectric constant of the soil (the soil volumetric water percentage). When a certain soil dielectric keeps constant, with the increase of *a*/*b* ratio, the capacity value of the micro-scale planar capacitance increases all the time. We analyzed adjacent two soils with different dielectric constants ($\varepsilon_4$=16.8 and $\varepsilon_5$=20.3), differential capacity values (*C*) of micro-scale planar capacitance of the probe are shown in Table 2. With the increase of *a*/*b* ratio, the difference of the capacity values of the micro-scale planar capacitance sensed between two adjacent soils increases. In other words, the difference values of capacitances sensed by the probe increases with the increase of *a*/*b* ratio under the condition that the volumetric water percentages of soil are different. The sensitivity of the sensor is the ratio of output variation and input variation caused. When the sensor probe in the research is used to moisture measurements of different soil, differential capacitance values express higher sensitivity. Therefore the sensitivity of the sensor is the higher with the increase of the ratio of *a*/*b*.

The sensitivity and detection range of the sensor probe are related to the ratio of *a*/*b*. If only consider the sensor sensitivity, the bigger the ratio of *a*/*b*, the greater the sensitivity of sensor probe. That is to say, when *b* is unchanged, the sensitivity of sensor probe increases with the increase of *a*. When only the detection range of the sensor probe was considered, the model of finite element analysis indicated that the detection range was the largest, when the size of *a* was 20 mm and the size of *b* was 10 mm. In addition, take into account of actual measurement requirement, the total size of the sensor probe is 100 mm. Taking sensitivity and detection range of sensor probe and measurement requirement into consideration, when the length of *a* is 20 mm and the length of *b* is 10 mm, the structure of sensor probe is optimal. The sensor is suitable for moisture measurement of different types of soil.

## 4 Results and discussion

### 4.1 Sensor calibration

Calibration is necessary for the design process of probe. In order to overcome the errors caused by differences in parasitic capacitance and the parameters of the oscillation circuit components, we did not adopt the absolute output frequency of the sensor, but the relative frequency shift index ($\eta = -\frac{F_A - F_S}{F_A - F_W}$) of the oscillating circuit in the calibration method of the sensor. $F_A$, $F_W$, and $F_S$ respectively indicated the output frequency of the sensor probe when it was put in air, water, and soil.

Standard farmland soil of National Precision Agriculture Demonstration Base locates in Xiaotangshan, Beijing was acquired. Under the laboratory environment, after being sieved and dried, 8 soil samples with different volumetric water percentages were prepared according to the volumetric weight of 1.35 g/cm$^3$. Then soil samples were evenly added into the containers where the sensor protective sleeve was installed in advance and sealed for 48 h until the soil moisture was balanced adequately. Each soil sample was measured five times. After removed the maximum value and the minimum value, the average values of other 3 measurements were calculated. Then the quadratic curve was fitted with the calculated values (Figure 7) and the correlation coefficient $R^2$ was 0.967.

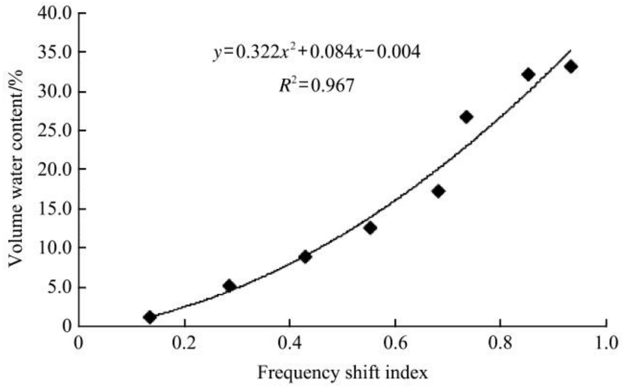


Figure 7 Calibration results of the sensor

## 4.2 Sensor stability test

Under the laboratory environment, four soil samples with different volumetric water percentages prepared according to the volumetric weight of 1.35 g/cm$^3$ were sealed for 48 h until the soil moisture was balanced adequately. Actual water percentage was measured using the standard drying method (oven drying method). Then one sensor probe was selected randomly to perform 10 h continuous measurement and the measurement results were recorded. In the measurement process with the sensor, soil samples were sealed. The stability test results of sensor probe are shown in Table 3. According to the experimental data, the maximum deviation of sensor is 0.28%, which indicates the high stability of sensor probe.

**Table 3 Soil moisture content of the sensor with different soil samples (%)**

| Measure time/h | Soil sample | | | |
|---|---|---|---|---|
| | 1 | 2 | 3 | 4 |
| 1 | 8.05 | 14.05 | 21.89 | 25.97 |
| 2 | 8.14 | 13.94 | 22.06 | 26.01 |
| 3 | 7.96 | 13.96 | 22.08 | 26.07 |
| 4 | 8.01 | 14.01 | 21.96 | 25.99 |
| 5 | 7.98 | 13.98 | 21.99 | 25.98 |
| 6 | 8.04 | 13.89 | 22.05 | 26.07 |
| 7 | 7.99 | 14.01 | 22.08 | 25.97 |
| 8 | 7.92 | 14.02 | 22.06 | 26.06 |

## 4.3 Sensor consistency test

The consistency is an important performance index for a sensor. Good consistency is the premise of standardization production and interchangeability of soil moisture sensor. In this research, the sensor was assembled with several sensor probes. Therefore, the consistency is particularly important. Three sensor probes were selected randomly to measure soil samples used in the stability test. Each soil sample was measured for five times. After removing the maximum value and the minimum value, the average values of other three measurements were calculated. The stability test results of the sensor probe are shown in Table 4. According to the data of experiment, the maximum deviation of the sensor was 1.57%, which indicated high consistency of the sensor probe.

**Table 4 Soil moisture content of different sensor probe with different soil samples (%)**

| Sensor probe Soil sample | 1 | 2 | 3 |
|---|---|---|---|
| 1 | 8.05 | 7.76 | 8.28 |
| 2 | 14.03 | 13.58 | 13.07 |
| 3 | 21.96 | 21.18 | 22.16 |
| 4 | 26.80 | 25.23 | 25.76 |

## 4.4 Sensor precision test

A piece of area with size of 3 m × 2 m was selected in the standard farmland of National Precision Agriculture Demonstration Base locates in Xiaotangshan in Beijing, it was segmented into six blocks. The area of each block was 1 m × 1 m. There is no moisture exchange between the blocks (Figure 8).

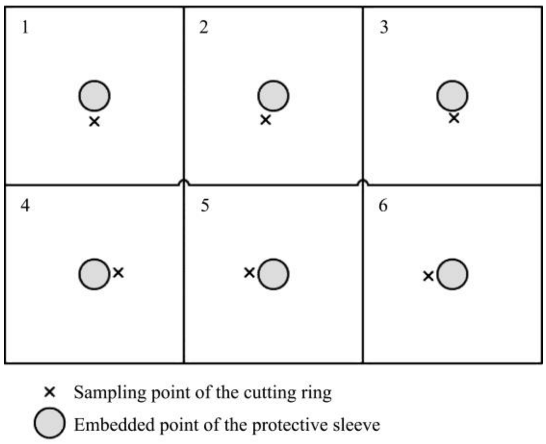


Figure 8 Locations of the sensors embedded and sampling points

The protective sleeve of the profile soil moisture sensor was embedded into soil at the center of each block to establish a good contact between the soil and the outer edge of protective sleeve. Then different volumes of water was injected into each block and covered with thin films in order to prevent the quick evaporation of moisture. Soil moisture percentage was measured after 72 h. Firstly, soil samples were obtained with a cutting ring in the area 5 cm away from the protective sleeve. The volumetric water percentage of the soil was calculated using the standard drying method. Then, the soil moisture sensor probe was put into the protective sleeve to measure the soil water percentage. The measured soil volumetric water percentages obtained by standard drying method were treated as the true values and the values measured with the sensor were treated as the observed values. Each measurement was repeated for five times and the results were averaged. For the convenience of calculation, the moisture percentages were multiplied by 100. The mean square error of the calculation results is 1.31 and the calculation results are shown in Table 2.

**Table 2 Comparison of moisture results obtained by standard drying method and profile soil moisture sensor**

| Test method | Soil sample 1 | Soil sample 2 | Soil sample 3 | Soil sample 4 | Soil sample 5 | Soil sample 6 | Mean Square Error |
|---|---|---|---|---|---|---|---|
| Standard Drying method | 7.56 | 10.32 | 15.68 | 18.56 | 23.72 | 28.26 | 1.31 |
| Profile soil moisture sensor | 6.53 | 11.26 | 13.89 | 19.36 | 24.68 | 30.14 | |

## 5 Conclusions

In this research, we analyzed the high frequency capacitance edge field effect principle and based on which designed a profile soil moisture sensor. Based on the theoretical study and the inference analysis of measurement mechanism of the sensor, we determined the key factors of profile soil moisture sensor. Through finite element analysis, we established two-dimensional trace planar capacitance probe model and determined the probe structure by analyzing the changing circumstances of the capacitance value and the electric field intensity around the trace planar capacitance probe. The design parameters of the probe which could get optimal sensitivity and detection range are: outer diameter 40 mm and inner diameter 38.4 mm of probe copper ring electrode, axial length 20 mm and axial spacing 10 mm. The sensor is suitable for moisture measurement of different types of soil and has a novel structure and a high waterproof grade. The sensor probe can be assembled variable according to the actual measurement depth in order to meet the soil moisture measurement requirements in different crop root zones. The measurement accuracy of the profile soil moisture sensor is ±1.31% and the sensor has better stability and consistency.

## Acknowledgments

We thank Beijing Natural Science Foundation (6142011) for supporting this research.

## [References]

[1] Luo X W, Zang Y, Zhou Z Y. Research progress in farming information acquisition technique for precision agriculture. Transactions of the CSAE, 2006; 22(1): 167–173. (in Chinese with English abstract)

[2] Fan J, Shao M G, Wang Q J. Development about methods of soil hydraulic conductivity determination in fields. Science of Soil and Water Conservation, 2006; 4(2): 114–119. (in Chinese with English abstract)

[3] Wang X L, Hu J D, Jiang M, Zhao X Y, Hu J F, Zhao Y Y. Experiment on fast-measurement of soil moisture based on additional resistance method. Transactions of the CSAE, 2009; 25(10): 76–81. (in Chinese with English abstract)

[4] Gaskin G J, Miller J D. Measurement of soil water percentage using a simplified impedance measuring technique. J Agric Eng Res, 1996; 63(1): 153–160.

[5] Rial W S, Han Y J. Assessing soil water percentage using complex permittivity. Transactions of the ASAE, 2000, 43(6): 1979–1985.

[6] Sun Y R, Dao-Kun M A, Lin J H, Lammers P S, Damerow L. An improved frequency domain technique for determining soil water content. Pedosphere, 2005; 15(6): 805–812.

[7] Bell J P, Dean T J, Hodnett M G. Soil moisture measurement by an improved capacitance technique, Part II: field techniques, evaluation and calibration. J. Hydrology, 1987; 93 (1): 79–90.

[8] Sun Y R, Ma D K, He Q, Zhao Y D. Experimental study of sensor for real-time measurement of soil moisture profile. Journal of Beijing Forestry University, 2006; 28(1): 55–59. (in Chinese with English abstract)

[9] Fan J, Shao M A, Wang Q J. Development about methods of soil hydraulic conductivity determination in fields.

Science of soil and Water Conservation, 2006; 4(2): 114–119. (in Chinese with English abstract)

[10] Xu L G, Yang J S, Xu N J, Hang Z. Progress of the study on theories and models of water-salt transport in cultivated soil. Arid Zone Research, 2004; 21(3): 254–258. (in Chinese with English abstract)

[11] Deng J C, Jiang X, Hu W P, Lu X, Wang F. Experimental investigation of atrazine transport in field soil profile. Transactions of the CSAE, 2008; 24(3): 77–81. (in Chinese with English abstract)

[12] Gao Y, Duan A W, Liu Z D, Wang H Z, Chen J P, Liu A N. Crop root growth and water uptake in maize/soybean strip intercropping. Chinese Journal of Applied Ecology, 2009; 20(2): 307–313. (in Chinese with English abstract)

[13] Hu J D, Zhao X Y, Li Z F, Wu J Z, Shi J H. Technique considerations on the use of a probe capacitance sensor with parameter modulation for measuring soil water percentage. Chinese Journal of Sensors and Actuators, 2007; 20(5): 1057–1060. (in Chinese with English abstract)

[14] Xu J H, Ma X Y, Sally D L, Horton R. FDR probe structure influence on the soil dielectric spectrum measurement. Transactions of the CSAM, 2014; 45(01): 102–107. (in Chinese with English abstract)

[15] Luo X W, Perumpral J V. Study on soil strength with microwave reflection loss. Transactions of the CSAE, 1995; 11(1): 46–51. (in Chinese with English abstract)

[16] Heimovaara T J, Winter E J G, Loon W K P, Esveld D C. Frequency dependent dielectric permittivity from 0 to 1 GHz: Time domain reflectometry measurements compared with frequency domain network analyzer measurements. Water Resource Research, 1996; 32(12): 3603–3610.

[17] Topp G C, Davis J L, Ann A P. Electromagnetic determination of soil water percentage: measurements in coaxial transmission lines. Water Resource Research, 1980; 16(3): 574–582.

[18] He Q Z, He J. The principle and application of a single planar capacitance sensor. Industrial Instrumentation & Automation, 2001; (5): 62–63, 58. (in Chinese with English abstract)

[19] Yang L, Mao Z H, Dong L L. Development of plane polar probe of capacitive grain moisture sensor. Transactions of the CSAE, 2010; 26(2): 185–189. (in Chinese with English abstract)